

## Reflection of traveling waves near the onset of binary-fluid convection

M. S. Bourzutschky and M. C. Cross

California Institute of Technology, Pasadena, California 91125

(Received 18 February 1992)

The reflection coefficient of linear traveling waves in binary-fluid convection is calculated for the experimental situation of rigid, impermeable boundaries. Results for a range of parameters of interest to experiments in ethanol-water mixtures are displayed and compared with experiment.

PACS number(s): 47.25.Qv, 47.20.Bp

### I. INTRODUCTION

Rayleigh-Bénard convection in binary fluids has been the subject of considerable experimental and theoretical attention as a convenient framework for studying a variety of nonequilibrium phenomena [1]. One of the interesting features of binary-fluid convection is that the primary instability in a thin horizontal layer of fluid mixture heated from below can be oscillatory, rather than stationary. Only recently has it been recognized experimentally [2] and theoretically [3] that an oscillatory instability at nonzero wave number can lead to traveling-wave states even in a laterally confined geometry, where one might have expected only standing-wave solutions. These traveling-wave states lead to the picture of a convection cell as a resonant cavity, in which the growth of the convective instability, as it travels through the cell, is balanced by losses upon reflection from the sidewalls. A smaller reflection coefficient  $r$  must be balanced by a larger growth rate in the bulk, and so suppresses the onset further from the ideal value in a laterally infinite system [4].

The reflection coefficient is therefore *the* additional parameter needed to characterize the onset of oscillatory convection in finite geometries, beyond the parameters one can obtain from calculations on horizontally unbounded systems [5]. Even for the linearized fluid equations, analytic solutions for  $r$  have only been found when unphysical free slip and permeable boundary conditions are imposed at the top and bottom plates [3,6]. In this paper, we introduce a numerical scheme that allows calculation of  $r$  for physically realistic boundary conditions, with relatively modest computational effort. These calculations now permit quantitative comparison with experimental results for the reflection coefficient, determined either from the suppression of the onset from the value calculated for the laterally infinite system, or from pulse propagation measurements. We concentrate on the *linearized* problem in this paper; current understanding of the weakly nonlinear case is much more rudimentary, some recent theoretical work is described in [6] and references therein.

### II. EQUATIONS OF BINARY FLUID CONVECTION

We study a binary fluid confined to a two-dimensional semi-infinite container, with coordinates  $-\frac{1}{2} \leq z \leq \frac{1}{2}$

and  $x > 0$ . The top and bottom horizontal container walls at  $z = \pm \frac{1}{2}$  are perfectly conducting and impermeable. At  $x=0$  the fluid is bordered by an impermeable sidewall extending to  $x=-d$ , with thermal properties to be specified. The sidewall is thermally insulated at  $x=-d$ . This model system resembles quite closely typical experimental situations.

Using the Boussinesq approximation, the linearized equations of motion can then be written [7] as

$$\begin{pmatrix} \nabla^2(\nabla^2 - \partial_t/\sigma) & (1 + \psi)\partial_x & -\partial_x \\ R\partial_x & \nabla^2 - \partial_t & 0 \\ 0 & \psi\nabla^2 & L\nabla^2 - \partial_t \end{pmatrix} \begin{pmatrix} \phi \\ \theta \\ \eta \end{pmatrix} = \begin{pmatrix} 0 \\ 0 \\ 0 \end{pmatrix}. \quad (2.1)$$

We have expressed the fluid velocity  $\mathbf{u} = (u, w)$  in terms of the stream function  $\phi$ , such that  $w = \partial_x \phi$  and  $u = -\partial_z \phi$ . The remaining fields of Eq. (2.1) are the deviation  $\theta$  of the temperature from the linear conducting profile, and  $\eta = c + \psi\theta$ , where  $c$  is the deviation of the concentration of the second component from the linear conducting profile driven by the Soret effect. The fluid parameters are the Prandtl number  $\sigma$  (ratio of thermal to viscous diffusivities), Lewis number  $L$  (ratio of impurity to thermal diffusivities), separation ratio  $\psi$  (giving the ratio of the importance of thermal and concentration buoyancy effects), and the Rayleigh number  $R$  giving in dimensionless form the driving temperature gradient.

The equations have been made dimensionless [7], so that time is measured in units of the vertical thermal diffusion time, and space is measured in terms of the vertical separation of the plates. The boundary conditions at the upper and lower plates are

$$\phi = \partial_z \phi = \theta = \partial_z \eta = 0, \quad z = \pm \frac{1}{2}. \quad (2.2)$$

At the sidewall, the boundary conditions read, for  $x=0$ ,

$$\begin{aligned} \partial_x \phi = \partial_z \phi = \partial_x \eta = 0, \\ \theta_f = \theta_w, \end{aligned} \quad (2.3)$$

$$\partial_x \theta_f = K_w \partial_x \theta_w,$$

and at  $x = -d$ ,

$$\partial_x \theta_w = 0. \quad (2.4)$$

The subscripts  $w$  and  $f$  refer to wall and fluid respectively, and  $K_w$  is the ratio of the thermal conductivity of the

sidewall material to the thermal conductivity of the fluid. As outlined in the Appendix, satisfying Eq. (2.3) introduces the additional parameter  $\kappa_w$ , the thermal diffusivity of the sidewall in units of the thermal diffusivity of the fluid.

### III. COMPUTATIONAL METHOD

We now describe a numerical procedure to solve Eq. (2.1). Following an algorithm applied to a similar problem in pure fluid convection [8], we assume that the solution of the semi-infinite system can be written as a superposition of eigenstates of the infinite system, with coefficients chosen to satisfy the boundary conditions at  $x=0$  and  $\infty$ .

A typical eigenstate, which we can assume to have even parity because of the  $z \leftrightarrow -z$  symmetry of the problem, is given by

$$\phi(x, z, t) = \exp(ikx) \sum_{j=1}^4 B_j \cosh(q_j z) \exp(-i\Omega t), \quad (3.1)$$

where  $q_j^2 = Q_j + k^2$ , and the  $Q_j$  are the four roots of the dispersion relation resulting from Eq. (2.1):

$$LQ^4 + i\Omega(1+L+L/\sigma)Q^3 - \Omega^2(1+1/\sigma+L/\sigma)Q^2 + [Rk^2(\psi+L+L\psi) - i\Omega^3/\sigma]Q + iRk^2\Omega(1+\psi) = 0. \quad (3.2)$$

$\Omega$  is a real frequency and  $k$  is a complex wave vector. Imposing the boundary conditions equation (2.2) leads to an additional constraint in the form of a vanishing complex determinant. The coefficients  $B_j$  in Eq. (3.1) are then determined up to an arbitrary multiplicative constant, which we fix by setting  $B_1 = 1$ .

Varying purely real  $k$ , there is a unique value  $k_c$  (up to a sign) at which  $R$  is minimized. This solution then defines the critical Rayleigh number  $R_c$  and the critical frequency  $\Omega_c$ . Once  $R_c$  and  $\Omega_c$  are determined, additional eigenstates can be found for an infinite but discrete set

$$\phi(x, z, t) = [\exp(-ik_c x) + r \exp(ik_c x)] \sum_{j=1}^4 B_{j1} \cosh(q_{j1} z) \exp(-i\Omega_c t) + \sum_{n=2}^N A_n \exp(ik_n x) \sum_{j=1}^4 B_{jn} \cosh(q_{jn} z) \exp(-i\Omega_c t). \quad (3.3)$$

The first term in Eq. (3.3) contains the traveling-wave components, consisting of an incident wave with amplitude 1 and a reflected wave with amplitude  $r$ . The second term contains the spatially localized components, which decay exponentially away from the sidewall with decay lengths given by the inverse of the imaginary parts of the wave vectors  $k_n$ . Denoting the wave vector with the smallest imaginary part as  $k_2$ , we estimate that our semi-infinite model calculations remain valid for finite systems of size  $\Gamma$ , as long as  $\Gamma \gg 2/\text{Im}(k_2)$ . In the infinite Prandtl number limit, we find  $\text{Im}(k_2) \approx 5|\psi|^{1/2}$ .

To determine the  $N$  unknowns  $r$  and  $A_n$  for  $n=2, \dots, N$ , we enforce the boundary conditions at  $x=0$  at a finite number of points  $M$  between  $z=0$  and  $z=\frac{1}{2}$ , with  $M=N/4$ . For simplicity, we choose the points spaced uniformly and enforce  $\partial_z \phi = 0$  at  $z=i/2(M+1)$ ,

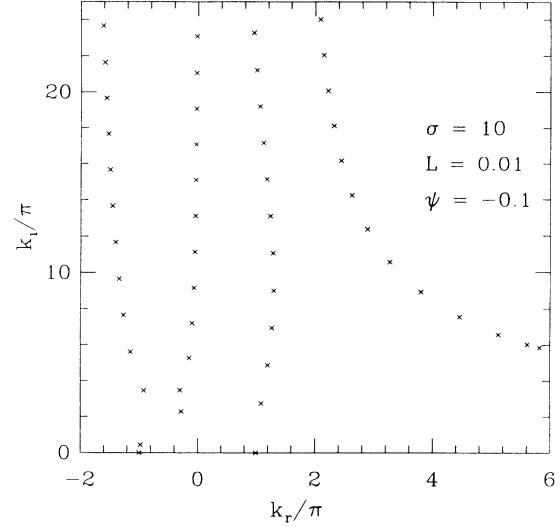


FIG. 1. Location of wave vectors  $k_n$  satisfying Eq. (3.1) in the complex plane.

of complex wave vectors  $k_n$ . These eigenstates decay exponentially away from the sidewall and therefore are not relevant to the laterally infinite system. For solutions to remain finite as  $x \rightarrow \infty$  in our semi-infinite system, only  $k_n$  with positive imaginary components are allowed. The boundary conditions render the equations transcendental, so that the solutions have to be found numerically.

A representative set of solutions is shown in Fig. 1. There are four branches of roots, resulting from the order of the dispersion relation Eq. (3.2). Asymptotically, the imaginary components within each branch differ by  $\approx 2\pi$ . Limiting forms for these roots are rather complicated and do not appear to be helpful in actual computations.

The eigenstates determined above have no obvious orthogonality properties, and so we truncate the expansion at a finite number of terms  $N$  and write

$\partial_x \phi = 0$  and the  $\theta$  boundary condition at  $z=(i-1)/2M$ , and  $\partial_x \eta = 0$  at  $z=(i-1)/2(M-1)$ , where  $i=1, \dots, M$ . The different choices arise because some of the conditions are satisfied automatically at  $z=0$  or  $z=\frac{1}{2}$  due to the symmetry of the expansion. Substituting these conditions into Eq. (3.3) finally results in  $N$  linear equations with  $N$  unknowns.

The convergence of Eq. (3.3) is quite rapid;  $r$  changes by less than 1% for  $M \geq 8$ . We also find that  $|A_n|$  decreases rapidly with  $n$ , i.e., approximately 4 orders of magnitude from  $n=1$  to 20, which justifies the ordering of the expansion. Finally, we have checked that the boundary conditions at  $x=0$  approach the correct values for points other than those that are explicitly matched, again finding rapid convergence.

IV. RESULTS

Using the method outlined in the previous section, we can now compute the reflection coefficient for several situations of interest. In Fig. 2(a) we show results for perfectly insulating sidewalls and a range of Prandtl numbers  $\sigma$ , in the limit of zero Lewis number  $L$ . To verify that the limit  $L \rightarrow 0$  is approached quite smoothly, we show  $r$  for  $\sigma=10$  and a range of  $L$  typical for ethanol-water mixtures, in the inset in Fig. 2(a). Only when  $|\psi| \sim L^2$  are significant differences seen between the curves. In fact, the equations become singular for a critical value  $\psi_c$  at which the group velocity  $s = \partial\Omega/\partial k$  goes through zero and changes sign. For  $\sigma=10$ , we find that  $\psi_c/L^2 \approx -0.70$  as  $L \rightarrow 0$ . By comparison, the codimension-2 point, where the transition to stationary convection occurs, is located at  $\psi/L^2 \approx -0.355$ . We have not investigated this singular

regime in further detail, as we expect nonlinearities and finite-size effects to play a significant role in typical experimental situations in this case.

In Fig. 2(b) we show  $r$  for a range of boundary conditions in the limit of a thick sidewall,  $d \gg 1$ . The main conclusion is that  $|r| \sim |\psi|^{1/2}$  for small  $|\psi|$ , as already predicted by calculations with free slip boundary conditions [3,6]. We also find that for  $\sigma \approx 10$ , typical for ethanol-water mixtures, the Prandtl number dependence becomes quite weak.

V. DISCUSSION

To conclude, we make a comparison with some experimental results [9] in Table I. The agreement for  $\psi = -0.558$  is excellent, but for smaller values of  $|\psi|$  there are systematic differences between experiment and theory. We also note that another experiment [10] was found to be consistent with a constant  $r$ , even down to  $|\psi|=0.01$ . The dependence of this consistency on the assumption for  $r$  has not been tested, and the identification of the laterally infinite  $R_c$  in [10] is indirect and may be suspect, although the qualitative dependence of  $r$  on the thermal conductivity of the sidewall found in [10] agrees with Fig. 2(b). Thus there is no experimental evidence for the expected  $|\psi|^{1/2}$  dependence. We hope that further experimental studies will provide a systematic test of our predictions.

ACKNOWLEDGMENTS

We would like to thank Eugenia Kuo for useful discussions. This work was partially supported by the National Science Foundation through Grant No. DMR-9013984.

APPENDIX

Here we describe how the thermal properties of the sidewall can be incorporated into the binary-fluid problem. The general solution of the heat equation for the temperature  $\theta_w$  in the sidewall, truncated to  $M$  terms, can be written as

$$\theta_w(x, z, t) = \sum_{n=1}^M c_n \cos(b_n z) \cosh[\lambda_n(x+d)] \times \exp(-i\Omega_c t), \tag{A1}$$

where

$$b_n = (2n-1)\pi, \quad \lambda_n = (b_n^2 - i\Omega_c/\kappa_w)^{1/2}. \tag{A2}$$

TABLE I. Comparison between experimental and theoretical values of the reflection coefficient  $|r|$ , for thick side walls.

$\psi$	$\sigma$	$K_w$	$\kappa_w$	$ r _{\text{expt}}$	$ r _{\text{theory}}$
-0.558	14.9	0.42	1.24	0.287	0.285
-0.437	19.6	0.45	1.31	0.305	0.277
-0.276	9.71	0.41	1.18	0.311	0.258
-0.262	11.9	0.43	1.25	0.294	0.253

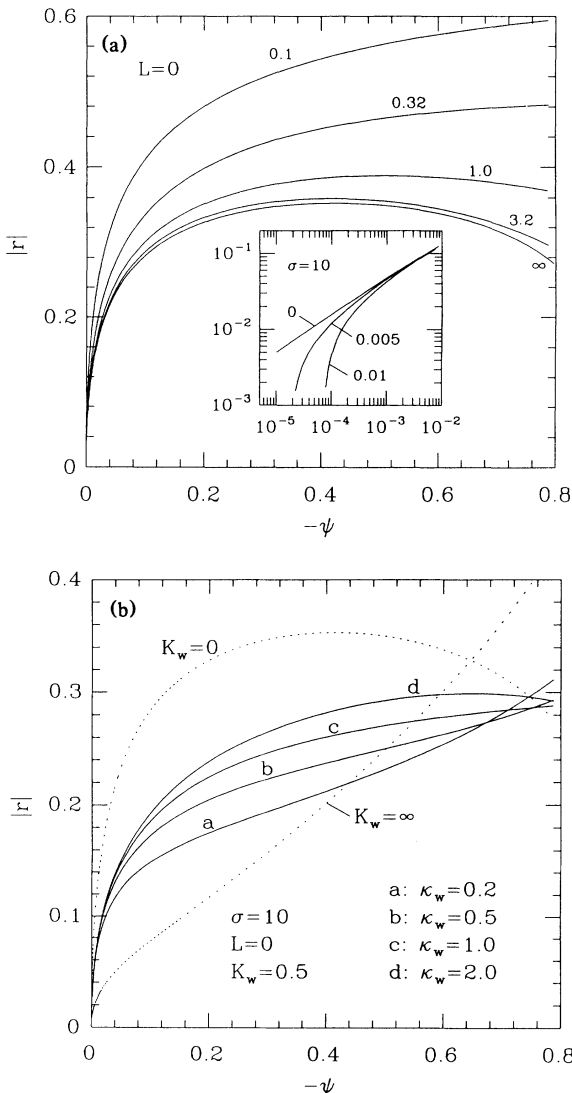


FIG. 2. The reflection coefficient  $|r|$  as a function of  $\psi$ . (a) Insulating sidewalls,  $\sigma=0.1, 0.32, 1.0, 3.2,$  and  $\infty$ , with  $L=0$ . The inset shows  $|r|$  for  $\sigma=10$  and  $L=0, 0.005,$  and  $0.01$ . (b)  $|r|$  for  $\sigma=10, L=0,$  and a range of thermal boundary conditions.

Matching Eq. (A1) to  $\theta_f$  using the boundary conditions Eq. (2.3) then allows elimination of the coefficients  $c_n$  from Eq. (A1). To state the result, it is convenient to introduce an  $M \times M$  matrix  $\underline{C}$  together with its inverse  $\underline{C}^{-1}$ , and an  $M \times N$  matrix  $\underline{D}$ :

$$C_{ij} = \cos(b_j z_i), \tag{A3}$$

$$D_{ij} = k_j \sum_{k=1}^M C_{ik}^{-1} \sum_{m=1}^4 \frac{B_{mj} \cosh(q_{mj} z_k)}{Q_{mj} + i \Omega_c}. \tag{A4}$$

Using these definitions, we finally obtain  $M$  equations for the  $N$  unknowns  $A_j$ :

$$\left( \lambda_i \tanh(\lambda_i d) - \frac{ik_j}{K_w} \right) D_{ij} A_j = \left( \lambda_i \tanh(\lambda_i d) + \frac{ik_1}{K_w} \right) D_{i1}, \tag{A5}$$

where  $A_1 = r$  and  $k_1 = k_c$ . In Eq. (A5) the index  $i$  runs from 1 to  $M$ , and  $j$  is summed from 1 to  $N$ .

In most cases it suffices to keep only the first term in Eq. (A1), which then simplifies the boundary condition to

$$\partial_x \theta_f + \beta \theta_f = 0, \tag{A6}$$

where  $\beta = -K_w \lambda_1 \tanh(\lambda_1 d)$ .

[1] For a review, see M. C. Cross and P. C. Hohenberg, *Rev. Mod. Phys.* (to be published).  
 [2] R. W. Walden, P. Kolodner, A. Passner, and C. M. Surko, *Phys. Rev. Lett.* **55**, 496 (1985).  
 [3] M. C. Cross, *Phys. Rev. Lett.* **57**, 2935 (1986).  
 [4] P. Kolodner, A. Passner, C. M. Surko, and R. W. Walden, *Phys. Rev. Lett.* **56**, 2621 (1986).  
 [5] M. C. Cross and Kihong Kim, *Phys. Rev. A* **37**, 3909 (1988); S. J. Linz and M. Lücke, *ibid.* **35**, 3997 (1987); E. Knobloch and D. R. Moore, *ibid.* **37**, 860 (1988); B. J. A.

Zielinski and H. R. Brand, *ibid.* **35**, 4349 (1987).  
 [6] M. C. Cross and E. Kuo (unpublished).  
 [7] D. T. J. Hurle and E. Jakeman, *J. Fluid Mech.* **47**, 667 (1971); D. Gutkowitz-Krusin, M. A. Collins, and J. Ross, *Phys. Fluids* **22**, 1443 (1979).  
 [8] K. Stewartson and M. Weinstein, *Phys. Fluids* **22**, 1421 (1979).  
 [9] P. Kolodner (private communication).  
 [10] J. Fineberg, E. Moses, and V. Steinberg, *Phys. Rev. A* **38**, 4939 (1988).